第 40 卷 第 4 期 焊 接 学 报 Vol. 40(4):050 − 054
2019 年 4 月 TRANSACTIONS OF THE CHINA WELDING INSTITUTION April 2019

滚动轧制对铝合金搅拌摩擦焊接头性能的影响

金玉花[1,2], 吴永武[1], 王希靖[1,2], 郭廷彪[1,2]

(1. 兰州理工大学 甘肃省有色金属先进加工与再利用省部共建国家重点实验室, 兰州 730050;
2. 兰州理工大学 材料科学与工程学院, 兰州 730050)

摘 要: 采用自制滚动轧制头对 5 mm 厚铝合金 7050 搅拌摩擦焊接头的上表面及背面进行滚动轧制, 并与其焊接态的接头作对比, 研究了滚动轧制对焊接接头性能的影响. 结果表明, 滚动轧制后接头表面的粗糙度由最大 9.58 μm 降低到平均约 0.85 μm. 表层发生了剧烈的塑性变形, 晶粒明显细化形成约 200 μm 厚的细晶层, 亚表层晶粒细化程度降低, 在焊核区伴有剪切带产生. 接头表层硬度明显提高, 其平均硬度高达 HV210, 相比轧制前硬度 HV110 提高了 91%. 接头表层残余应力由原来的拉应力转变为压应力, 最大残余压应力场深度约为 200 μm. 疲劳源由表层移至亚表层, 疲劳寿命显著提高.

关键词: 铝合金 7050; 搅拌摩擦焊; 滚动轧制; 组织; 力学性能

中图分类号: TG 456 **文献标识码:** A **doi:** 10.12073/j.hjxb.2019400099

0 序 言

搅拌摩擦焊 (FSW) 连接作为一项固态连接技术, 解决了铝合金、镁合金等各种难以熔焊连接材料的可靠连接难题[1]. 但是搅拌摩擦焊接头表面较大的粗糙度使得疲劳微裂纹极易在表面产生, 失稳向接头内部扩展致使接头失效. 因此针对搅拌摩擦焊接头强化研究, 国内外科研工作者引入超声喷丸、激光喷丸、表面碾压、超声表面轧制技术等[2-5]物理表面改性技术, 以及接头涂层[6]、渗碳、渗氮等表面化学改性方法尝试进一步改善接头性能. 郝宗斌等人[4] 采用多重旋转碾压对铝合金 FSW 焊缝进行了碾压, 表层晶粒明显细化, 硬度也大幅度升高, 组织和硬度均沿着接头厚度方向呈一定梯度分布; Hatamleh 等人[5]将激光喷丸、传统喷丸和超声喷丸对 AA2024 和 AA7075 FSW 接头的强化做了对比, 研究了喷丸对基体表面改性的影响, 表明激光喷丸增加了表层残余压应力场深度, 疲劳裂纹抗力进一步提高; Li 等人[6] 研究了表面冷喷涂对 AA2024-T3 搅拌摩擦焊接头的影响, 表面粗糙度显著降低, 残余压应力移向涂层, 拉伸性能和疲劳寿命分别增加 7% 和 4 倍. 针对以上技术的不足, 即在 FSW 接头喷丸过程中喷丸介质高速撞击试件表面, 在表面及次表面引入了残余压应力, 提高了接头疲劳性能, 但增加了接头表面粗糙度, 疲劳微裂纹极易在喷丸留下的凹坑边缘或沟犁内萌生并向次表层扩展[7]; 碾压由于飞边的存在使得焊缝和母材 (不在同一平面) 受压力不均; 在喷涂过程中涂层与接头界面处存在结合较差, 而且接头表面晶粒容易在喷涂过程中长大粗化. 试验中采用的滚动轧制方法可以解决这些不足, 在搅拌摩擦焊接基础上, 通过快速滚动轧制的施加重复载荷的方法[8], 旨在向表层引入了较大残余压应力的同时降低接头表面粗糙度, 其次用冷加工细化表层晶粒, 达到提高铝合金接头表面强度, 改善整个焊缝接头性能的目的.

1 试验方法

试验采用转速为 800 r/min, 焊接速度为 90 mm/min 的优化组合工艺参数对 5 mm 厚的铝合金 7050 退火态板材进行搅拌摩擦对接焊, 焊接完成后冷却到室温, 用细铁刷除去焊接时留下的毛刺及飞边, 用粗砂纸打磨接头表面, 在焊缝表面涂覆一层高温润滑油. 采用表 1 所示工艺参数进行旋转滚动轧制. 滚动轧制头及轧制示意图如图 1 所示. 用粗糙度仪 Mitutoyo SJ-201P 测量轧制前后焊缝表面粗糙度. 用线切割机垂直于焊缝截取尺寸为 25 mm ×

收稿日期: 2017 − 11 − 20

基金项目: 国家自然科学基金项目 (51865028); 甘肃省高等学校基本科研业务费 (01-0071); 兰州理工大学博士基金 (01-0765)

15 mm × 5 mm 的试样若干，金相试样制备好后，用 kellor 试剂 (HF：HCl：HNO_3：H_2O = 2：3：5：190) 进行金相腐蚀. 采用 OLYMPUSGX51 金相光学显微镜、Quanta FEG-450 扫描电镜 (SEM)、HV-1000B (100gf，加载 15 s) 数字维氏显微硬度仪对接头横截面分别进行宏观及微观组织形貌观察和硬度测试. 对轧制前后的试样逐层电解抛光 (电解液为 A2，电压为 20 kV)，用 X 射线衍射仪 (Rigaku) 获取每层应力值. 采用 MTS 810 Material Test System 试验机对哑铃状试样进行高周疲劳测试，加载频率为 50 Hz.

表 1　铝合金 7050 搅拌摩擦焊接头旋转滚动轧制工艺参数

Table 1　Rotation rolling experimental program of aluminum 7050 FSWed joint

转速 n/(r·min^{-1})	前进速度 v/(mm·min^{-1})	倾斜角 θ/(°)	下压量 L/mm
350	50	0.5	0.5

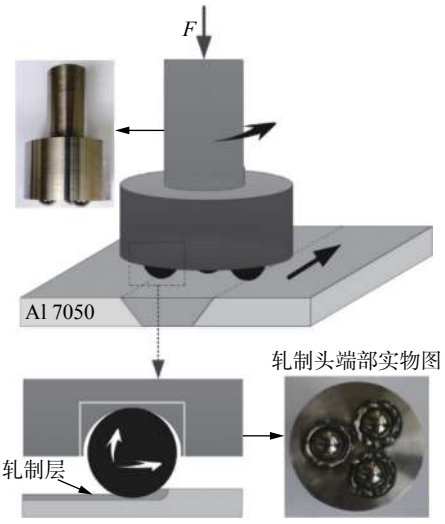

图 1　滚动轧制工作原理示意图及其实物图

Fig. 1　Working principle schematic of rolling and physical map

2　试验结果与分析

2.1　接头滚动轧制后表面粗糙度

对铝合金 7050 进行搅拌摩擦焊连接，剔除飞边后在接头表面的前进侧、中间和后退侧进行三道滚动轧制. 表面粗糙度测试结果显示轧制后的接头表面粗糙度降低，如图 2 所示. 轧制前的焊缝表面粗糙度 (R_a) 约为 9.58 μm，轧制后粗糙度 (R_a) 降低到 0.85 μm，表明滚动轧制显著提高了焊缝表面的光洁度.

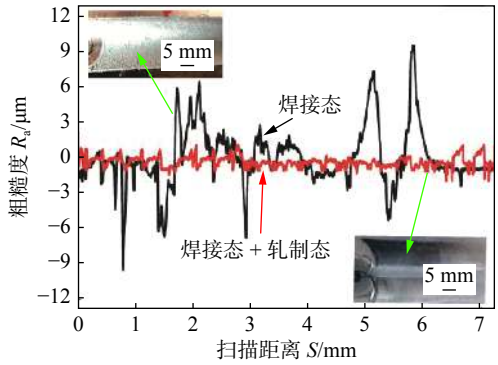

图 2　滚动轧制前后接头表面粗糙度

Fig. 2　Comparation of roughness before and after rolled FSW surface

2.2　轧制前后组织对比

对铝合金 7050 搅拌摩擦焊接头滚动轧制前后的表层组织进行对比分析，如图 3 所示. 图 3a 为接头焊接态横截面表层及亚表层焊核区组织，图 3b 为接头轧制后横截面表层及亚表层焊核区组织. 焊接态接头焊核区组织从焊缝表面沿厚度方向分别为紊流区、搅拌区，紊流区晶粒细小但厚度不均匀，焊核区较厚，焊核区两侧的热力影响区紊流区急剧减薄至消失. 搅拌区金属塑性变形金属经历了回复和动态再结晶，形成了较细的等轴晶. 接头表层组织实际由焊核区的紊流组织和热力影响区组织构成，热力影响区由于第二相的贫乏[9] 往往成为接头的薄弱区. 接头表面经过滚动轧制后，焊缝表层冷轧变形，一方面表层粗晶组织经过不同方向剧烈塑性变形使得原有的小角度晶界形成大角度晶界，逐渐细化为超细晶；另一方面，轧制过程中钢球与轧制表面接触点周围产生瞬时切应力，当达到临界分切应力时对应的滑移系开动发生塑性变形. 高速旋转滚动轧制使得表层晶粒的其它滑移系开动，不同滑移面上的新位错大量增殖、相互交割、攀移，位错

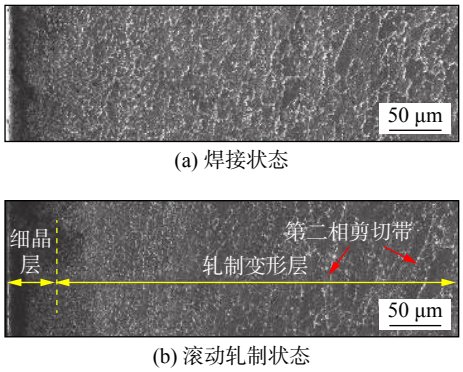

图 3　搅拌摩擦焊接头经过轧制前后的近表层微观组织

Fig. 3　Surface microstructure of aluminum 7050 FSWed joint after and before rolling

密度升高. 另外, 亚表层的晶粒内产生多系滑移及孪生, 使得沿厚度方向晶粒产生细化, 出现明显的伴有剪切带 (shear bands) 产生的轧制变形区, 强化相沿着剪切带晶界分布. 表层及亚表层总厚度大约 700 μm, 未变形部分的晶粒保持原有的焊核区晶粒形貌. 因此接头上下表层达到细晶强化及位错强化, 形成一个上下细晶层、内部粗晶的“Sandwich”梯度结构.

2.3 接头显微硬度

为了进一步探究滚动轧制对接头硬度的影响, 在沿厚度方向以焊缝为中心, 面积为 4.8 mm × 25 mm 的区域进行显微硬度测量并绘制二维云图, 如图 4a 所示. 图 4a 为焊接态接头截面的硬度分布. 接头横截面硬度整体分布不对称, 从前进侧 (AS) 的母材–热影响区–热力影响区–焊核区–后退侧 (RS) 的热力影响区–热影响区–母材, 接头水平硬度分布大致呈“锯齿形”.

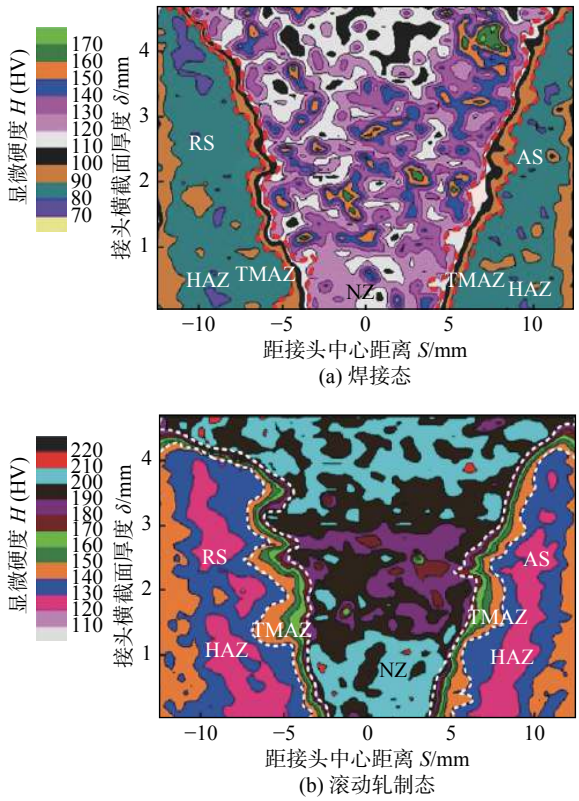

图 4 接头滚动轧制前后横截面硬度分布云图

Fig. 4 Microhardness contour chart of FSWed joint in cross section before (a) and after rolling (b)

两侧母材的硬度在 HV 100 ~ 110 范围. 热影响区硬度范围较宽, 后退侧所占面积更大, 硬度值在 HV 80 ~ 90 之间. 原因是后退侧热影响区晶粒在搅拌摩擦焊热循环下所受的热作用比前进侧大[10], 晶粒容易粗化且面积较大. 热力影响区 (虚线内) 范围较窄 (约 1 mm), 硬度值范围在 HV 100 ~ 120 之间, 该区域晶粒受热循环和热变形双重作用, 晶粒被拉伸变形, 硬度值高于热影响区. 焊核区硬度值呈现不均匀现象, 硬度在 HV 90 ~ 170 间变化. 这是由于在搅拌摩擦焊过程中该区域经历了剧烈的塑性流动和摩擦焊热循环, 晶粒发生了动态再结晶, 形成了细小的等轴晶. 同时在焊接过程中焊核区沉淀相重溶后析出发生了团聚, 沉淀相形状、分布均发生了改变, 致使接头发生了软化[11]. 因此在接头细晶强化和沉淀相分布不均匀作用下, 焊核区的硬度分布出现了不均匀的现象, 但整体硬度偏高.

图 4b 为图 4a 的接头上滚动轧制后得到的硬度分布. 接头的各区域的硬度相比焊接态接头都有不同程度的提高. 焊核区的表面及次表面硬度提高最显著, 形成了硬度值在 HV 190 ~ 220 范围的硬化层, 硬化层深约为 1.5 mm. 热力影响区 (白色虚线内) 硬度值横截面上的变化由焊接态的两层 (图 4a) 变为轧制态的四层 (图 4b) 过渡, 硬度变化较平缓. 此外, 该区域在板材厚度方向硬度变化更明显, 基本都在 HV 200 以上. 焊缝表面轧制改性后表层晶粒细化. 由 Hall-Patch 公式[12] 可知, 单位体积内晶粒尺寸减小, 晶界面积剧增, 轧制变形产生的新位错运动受阻形成位错塞积, 产生了应变硬化. 因此, 由滚动轧制后引起的应变硬化和细晶强化共同作用提高了接头表层及次表层的硬度.

2.4 接头残余应力分布

滚动轧制 FSW 接头改善了表层的应力分布. 图 5 为焊接态和滚动轧制后沿厚度方向近表层的残余应力分布. 对于 FSW 焊接态残余应力呈拉应力状态, 在距离接头表面 280 μm 处残余应力最大,

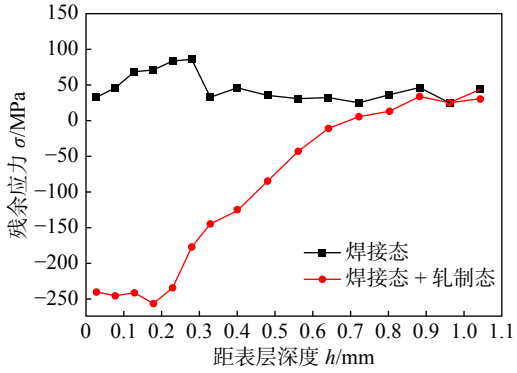

图 5 FSW 接头轧制前后表层残余应力分布

Fig. 5 Residual stresses distribution of aluminum 7050 FSWed joint after and before rolling

约 85 MPa, 沿着厚度的增加残余拉应力值递减. 初始拉应力值相对偏大可能由于焊接过程中焊接夹具控制使得试样无法靠变形释放热应力或是试样制备过程机械加工时引入的残余应力. 对于滚动轧制态, 在距离表面约 180 μm 处压应力呈现最大值为−260 MPa, 残余压应力场深度约为 700 μm. 沿接头厚度的增加, 在约 700 μm 处残余应力状态由压应力逐渐向拉应力过渡.

2.5　接头疲劳性能

经过滚动轧制 FSW 接头的疲劳寿命显著提高, 如图 6 所示. 在应力幅为 25 MPa, 最大应力与最小应力的比值 R 为−1, 加载频率 50 Hz 疲劳条件下, 焊接态接头疲劳寿命为 3.56×10^5 循环, 而滚动轧制后疲劳寿命达到 2.18×10^6 循环.

焊接态接头疲劳试验中断裂于前进侧热力影响区或者热影响区 (图 7a), 失稳于热影响区是由于热影响区晶粒粗化软化造成的; 失稳于热力影响区是由于热力影响区粗大的变形晶粒与焊核区等轴晶组织的显著差异以及热影响区强化相强化相再分配导致强化相出现贫乏, 微裂纹容易在此处扩展; 再者接头表层存在一定的焊接拉应力, 促使表面裂纹萌生扩展. 经过滚动轧制的接头在疲劳试验中断裂位置集中在后退侧的热影响区 (图 7c). 分析疲劳断裂位置改变的原因, 一方面轧制后焊缝表面产生了一定深度的硬度层, 提高了疲劳微裂纹扩展抗力, 焊接态时硬度较低的热影响区不直接暴露在表面; 另一方面轧制后接头表面的应力由焊接时拉应力转为压应力, 阻碍了疲劳裂纹扩展. 从图 7b, 7d

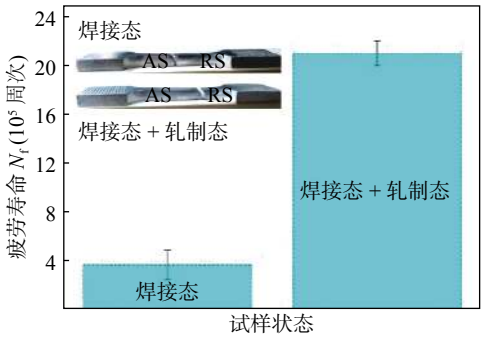

图 6　FSW 接头轧制前后拉-压疲劳寿命对比

Fig. 6　Comparations of tensile-pressure fatigue life under aluminum 7050 FSWed joint after and before rolling

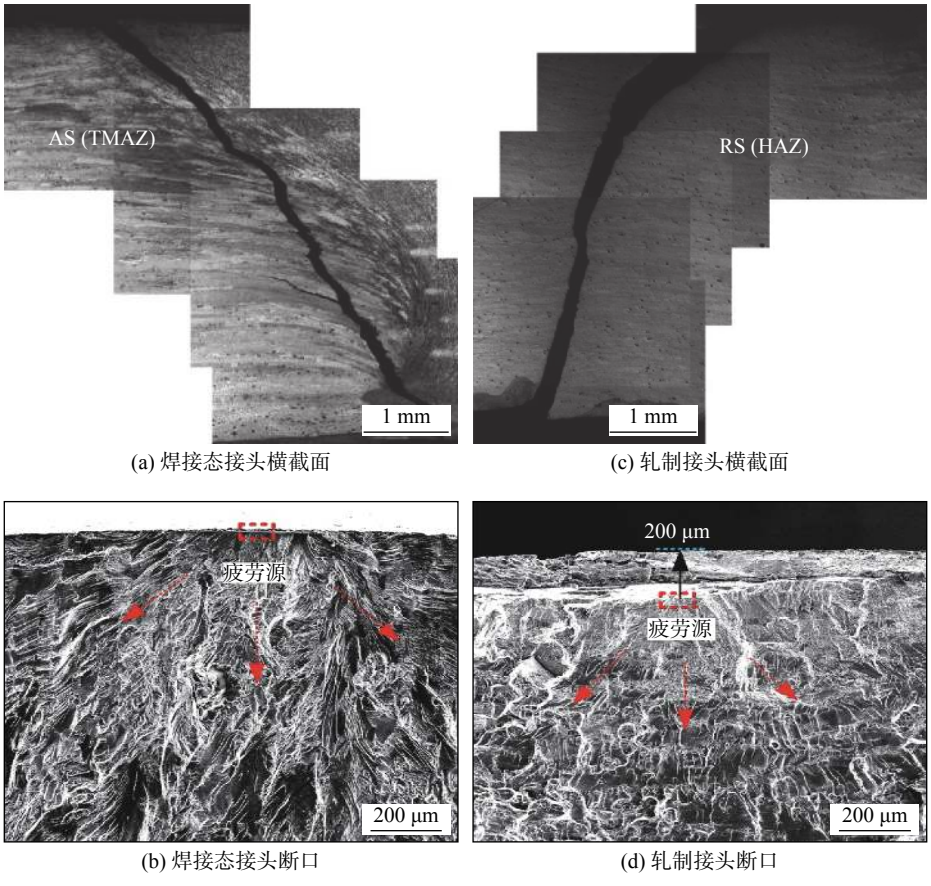

(a) 焊接态接头横截面　(c) 轧制接头横截面

(b) 焊接态接头断口　(d) 轧制接头断口

图 7　FSW 接头轧制前后疲劳断口形貌

Fig. 7　Fatigue fracture morphology under aluminum 7050 FSWed joint after and before rolling

疲劳断口的疲劳裂纹扩展区可以看出，接头滚动轧制后疲劳源向次表层迁移了约 200 μm，并形成了疲劳台阶. 疲劳源萌生后疲劳裂纹扩展形成了扇形状贝壳纹扩展区[13]. 而 FSW 接头的疲劳源在其表面，相应地形成了一定面积的疲劳扩展区. 可见，旋转滚动轧制改善了 FSW 接头疲劳性能.

3 结 论

(1) 试验探究了铝合金 7050 搅拌摩擦焊接头滚动轧制强化的规律：表层金属在轧制头挤压作用下发生塑性变形，晶粒间产生大量位错，位错之间相互作用，使得小角度晶界变为大角度晶界，形成小晶粒. 从表层到内部形成由细晶到粗晶的梯度分布.

(2) 接头整个区域轧制前后硬度分布不对称，轧制后接头的母材区、热影响区、热力影响区以及焊核区的硬度值都有不同程度的提高；焊核区硬度变化最明显，提高了约 95 HV. 轧制塑性变形层深度约 700 μm.

(3) 接头轧制前表层处于拉应力状态，滚动轧制向表层引入了残余压应力，阻碍了接头表面疲劳裂纹的扩展，最大残余压应力为 260 MPa.

(4) 接头经滚动轧制后疲劳寿命显著提高，疲劳源萌生位置移向次表层约 200 μm 处.

参考文献：

[1] Wu L H, Wang D, Xiao B L, *et al*. Microstructural evolution of the thermomechanically affected zone in a Ti–6Al–4V friction stir welded joint[J]. Scripta Materialia, 2014, 78(5): 17 − 20.

[2] Wang T, Wang D P, Liu G, *et al*. Investigations on the nanocrystallization of 40Cr using ultrasonic surface rolling processing[J]. Applied Surface Science, 2008, 225(5): 1824 − 1829.

[3] 解瑞军, 邱小明, 陈芙蓉, 等. 超声冲击实现 7A52 铝合金焊接接头表面纳米化 [J]. 焊接学报, 2014, 35(12): 35 − 38.
Xie Ruijun, Qiu Xiaoming, Chen Furong, *et al*. Surface nanocrystallization of 7A52 aluminum alloy welded joint using ultrasonic impact treatment[J]. Transactions of the China Welding Institution, 2014, 35(12): 35 − 38.

[4] 郝宗斌, 李晓泉, 李 阳, 等. 多重旋转碾压对铝合金搅拌摩擦焊缝表面的影响 [J]. 焊接学报, 2017, 38(2): 125 − 128.
Hao Zongbin, Li Xiaoquan, Li Yang, *et al*. Effect of multiple rotary rolling on the surface of friction stir weld of aluminum alloy[J]. Transactions of the China Welding Institution, 2017, 38(2): 125 − 128.

[5] Hatamleh O. A comprehensive investigation on the effects of laser and shot peening on fatigue crack growth in friction stir welded AA2195 joints[J]. International Journal of Fatigue, 2009, 31(5): 974 − 988.

[6] Li W Y, Li N, Yang X W, *et al*. Impact of cold spraying on microstructure and mechanical properties of optimized friction stir welded AA2024-T3 joint[J]. Materials Science & Engineering A, 2017, 702: 73 − 80.

[7] Wagner L, Mhaede M, Wollmann M, *et al*. Surface layer properties and fatigue behavior in Al 7075-T73 and Ti-6Al-4V: comparing results after laser peening: shot peening and burnishing[J]. International Journal of Structural Integrity, 2011, 2(2): 185 − 199.

[8] Chui P F, Suna K N, Suna C. Effect of surface induced by fast multiple rotation rolling on hardness and corrosion behavior of 316L stainless steel[J]. Applied Surface Science, 2011, 257(15): 6787 − 6791.

[9] 金玉花, 霍仁杰, 王希靖, 等. 旋转速度对 7055 铝合金搅拌摩擦焊接头断裂特征的影响 [J]. 焊接学报, 2017, 38(2): 10 − 13.
Jin Yuhua, Huo Renjie, Wang Xijing, *et al*. Effect of rotation speed on fracture characteristics of 7055 aluminum alloy friction stir welding joint[J]. Transactions of the China Welding Institution, 2017, 38(2): 10 − 13.

[10] Fu R, Sun Z, Sun R, *et al*. Improvement of weld temperature distribution and mechanical properties of 7050 aluminum alloy butt joints by submerged friction stir welding[J]. Material and Design, 2011, 32(10): 4825 − 4831.

[11] Sato Y S, Kokawa H. Distribution of tensile property and microstructure in friction stir weld of 6063 aluminum[J]. Metallurgical and Materials Transactions A, 2001, 32(12): 3023 − 3031.

[12] 石德珂. 材料科学基础 [M]. 北京: 机械工业出版社, 2005.

[13] Donald R. Askeland P P. The science and engineering of materials, fouth edition[M]. Beijing: Tsinghua University Press, 2005.

第一作者简介：金玉花，女，1971 年出生，博士，副教授. 主要从事有色金属及其合金的连接技术. 发表论文 20 余篇. Email: yhjin8686@163.com

Firstly, line by line search was carried out towards X-ray detection images of weldments left turning or right turning, and the unilateral projection overlap defects were found by using the method of the same distance from defect center point to the upper end of the image, then the depth location of overlap defects were judged by comparing the left or right projection distance of unilateral projection overlap defects, and the overlap defects were discriminated. The automatic discrimination of unilateral projection overlap defects in actual weldments was carried out, and the experimental results show that the provided method is feasible.

Key words: double T style weldments; multi-view images; unilateral projection; overlap defect; discrimination method

Effect of rolling on friction stir welded joints of aluminum alloy JIN Yuhua[1,2], WU Yongwu[1], WANG Xijing[1,2], GUO Tingbiao[1,2] (1. State Key Laboratory of Advanced Processing and Recycling of Non-ferrous Metals, Lanzhou University of Technology, Lanzhou 730050, China; 2. Material Science and Engineering Institute, Lanzhou University of Technology, Lanzhou 730050, China). pp 50-54

Abstract: The upper and back surface of a friction stir welded joint of 5 mm thick 7050 aluminum alloy were rolled by a self-made rolling head. It was compared with the welded joints without rolling. The effect of rolling on the performance of welded joints was studied. The results showed that the roughness of joint surface was reduced from 9.58 μm (maximum value) to 0.85 μm (mean value). The surface layer happened severe plastic deformation, and the grains were remarkably refined to form a fine grain layer of about 200 μm thick. The grain refinement of the subsurface layer was reduced, and a shear band was generated in the weld nugget zone. The hardness of the joint surface was obviously improved, and the average hardness was as high as HV210, which was 91% higher than the hardness HV110 before rolling. The residual stress of the joint surface changed from the original tensile stress to the compressive stress, and the maximum residual compressive stress field depth was about 200 μm. The source was moved from the surface layer to the subsurface layer, and the fatigue life was significantly improved.

Key words: 7050 aluminum alloy; friction stir welding; rolling; microstructure; mechanical properties

Microstructures and properties of friction stir welds of C18000 copper alloy HE Diqiu[1,2], MA Li[1], SUN Youqing[2], LAI Ruilin[2] (1. Light Alloy Research Institute, Central South University, Changsha 410083, China; 2. State Key Laboratory of High Performance Complex Manufacturing, Central South University, Changsha 410083, China). pp 55-60

Abstract: C18000 copper alloy plate with thickness of 3.5 mm was subjected to friction stir welding experiment. Sound welded joints were obtained under the welding speed of 120 mm/min and the rotation speed of 1 200 r/min. The macro-morphology and micro-structure of the joint were observed under metallographic microscope, and the microstructure of the base metal and stirring zone were observed and analyzed by scanning electron microscopy and transmission electron microscopy. The results showed that the joint zone could be generally divided into the base metal (BM), the heat affected zone (HAZ), the thermo-mechanically affected zone (TMAZ) and the stir zone (SZ). The grain in SZ was small and well-distributed, and the grain in TMAZ was elongated along the tangential direction of the boundary. It was found that the particles were Cr_3Si phase, and it was dissolved in the stirring zone. The Cr element phase and Ni_2Si phase dissolved in the microstructure of SZ, which resulted in a decrease in joint hardness and tensile strength. The average hardness of the SZ was 151.4 HV; the tensile strength of the joint was 497 MPa, which was 72% of the BM. The conductivity of the joint dropped to 35% IACS.

Key words: C18000 copper alloy; microstructure; TEM; mechanical properties; conductivity

Process characteristics of laser scanning welding of aluminum alloy HUANG Ruisheng[1], ZOU Jipeng[1], MENG Shenghao[2], YANG Yicheng[1], ZHANG Meiwei[1] (1. Harbin Welding Institute Limited Company, Harbin 150028, China; 2. State Key Laboratory of Advanced Welding and Joining, Harbin Institute of Technology, Harbin 150001, China). pp 61-66

Abstract: In order to reduce welding defects and improve the stability of the welding process during 6061 aluminum alloy laser welding, the high power solid state laser weaving welding technology was developed. The results showed that the higher quality welding seam could be obtained when the weaving range was 0.5 ~ 0.7 mm and the weaving frequency was 100 ~ 200 Hz. Laser weaving welding could significantly inhibit the generation of plasma and its size was 2/3 of the conventional laser welding, its area standard deviation was 1/2 of the conventional laser welding. Compared with the conventional laser welding technology, laser weaving welding could maintain a stable molten pool shape, where the keyhole moved steadily along the counter clockwise direction, and the keyhole area was about twice of the conventional laser welding.

Key words: laser technology; laser weaving welding; aluminum alloy; seam formation; welding stability

Theoretical study on dust distribution of multiple dust sources in welding workshop JIANG Zhongan, LAN Gui, PENG Ya (School of Civil and Resource Engineering, University of Science and Technology Beijing, Beijing 100083, China). pp 67-72

Abstract: In order to treat the dust in the welding